*36th EPS Conference on Plasma Phys. Sofia, June 29 - July 3, 2009 ECA Vol.**33E**, P-4.174 (2009)*

GLOBAL CONFINEMENT IN NBI PLASMAS OF THE TJ-II STELLARATOR UNDER LITHIUM-COATED WALL CONDITIONS

E. Ascasíbar, T. Estrada, M. Liniers, M. Ochando, F. L. Tabarés, D. Tafalla, J. Guasp, R. Jiménez-Gómez, F. Castejón, D. López-Bruna, A. López-Fraguas, I. Pastor, A. Cappa, C. Fuentes. J.M. Fontdecaba and the TJ-II Team

Laboratorio Nacional de Fusión, Asociación EURATOM-CIEMAT para Fusión. Madrid, Spain

Introduction

Earlier experimental studies in low density ($0.4\times10^{19}m^{-3} \le \bar{n}_e \le 1.2\times10^{19}m^{-3}$) ECH, boron-coated wall plasmas of the TJ-II stellarator (B ≈ 1 T, R = 1.5 m, <a> ≤ 0.22 m, $0.9 < \iota/2\pi(0) < 2.2$) yielded dependencies of the global energy confinement on operational parameters (plasma radius, heating power, density, rotational transform) in rough agreement with the ones obtained from stellarator inter-machine scaling studies, like ISS04 [1, 2]. Subsequent local transport studies extracted dependencies of the thermal diffusivity on the mentioned parameters, which confirmed and qualified the results of the global 0-dimensional study [3].

During 2008, NBI operation under lithium-coated wall has given access to a new operational regime as compared to the previous NBI plasmas with boron-coated wall. This new NBI scenario is characterized by enhanced, long-lasting density control, impurity reduction and improved confinement [4, 5]. The details of the lithiumization process and the physics behind the observed boosted performance are described in these references.

The present analysis concentrates in the global confinement of a set of 343 plasma discharges with pure NBI heating produced in 2008. The lithium wall plasma performance of an appropriate subset of discharges is compared to a set of boron wall NBI discharges produced in 2007 with one neutral beam injector.

Experimental data and computed parameters

TJ-II plasmas are always started up with ECR heating (two 53.2 GHz gyrotrons, 300 kW each, 2nd harmonic, X-mode polarization) to form a suitable target plasma for the subsequent neutral hydrogen beam injection. Typical values of the ECRH target density (line average) are in the range $0.5-0.8\times10^{19}m^{-3}$. The NBI system consists of two tangential injectors, co and counter, of hydrogen neutrals with beam energy ≤ 32 kV, current ≤ 60 A, port-through power ≤ 550 kW and pulse length ≤ 130 ms.

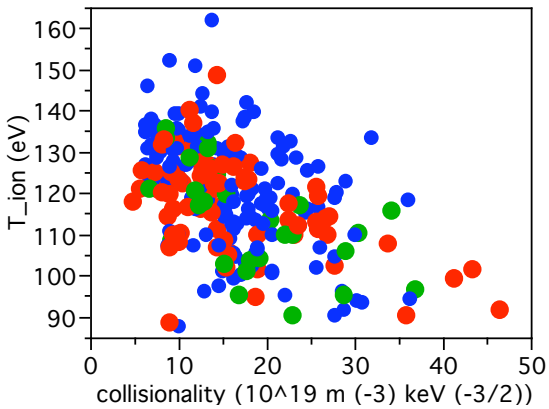

Figure 1: Central ion temperature vs. plasma collisionality for the three types of NBI heating: co- (red), counter (green) and both injectors (blue symbols).

Figure 1 shows that the ion temperature of the data cloud in the NBI phase has a small decreasing trend with plasma collisionality in the studied density range, 2-6 x 10^{19} m^{-3}, and is weakly dependent on the amount of applied heating power (one or both injectors). This fact can be understood considering the relatively small fraction of NBI heating power absorbed directly by the ions, typically, 28% [6]. Thus, doubling the injected heating power

allows accessing higher densities but also increases the electron temperature (the average relative increment, ΔT_e, being up to 30% at 5 x 10^{19} m^{-3} -from 0.27 to 0.35 keV) and produces only a marginal increment in overall collisionality.
Plasma energy content measured with the diamagnetic loop, W_dia, is the main magnitude, besides absorbed power, needed to quantify the energy confinement time, tau_E. Measured values of stored energy are up to 4.7 kJ. W_dia values are typically 50% larger than the thermal values, W_th, obtained from the integration of the Thomson Scattering diagnostic profiles. This discrepancy between both measurements decreases with increasing density and is not fully explained. It must be noted that, in the calculation of the thermal ion contribution to W_th for these NBI plasmas, the ion temperature is assumed to have the same radial profile as the electron temperature one. This was not the case for ECH plasmas, where we assumed profile similarity between ion density and electron temperature profiles and the ion contribution represented a fraction of 15% of the total energy content [1]. For the NBI plasmas studied in this work, considering a typical value of Zeff ≈ 1.5, the ion share increases to values around 30% [7].

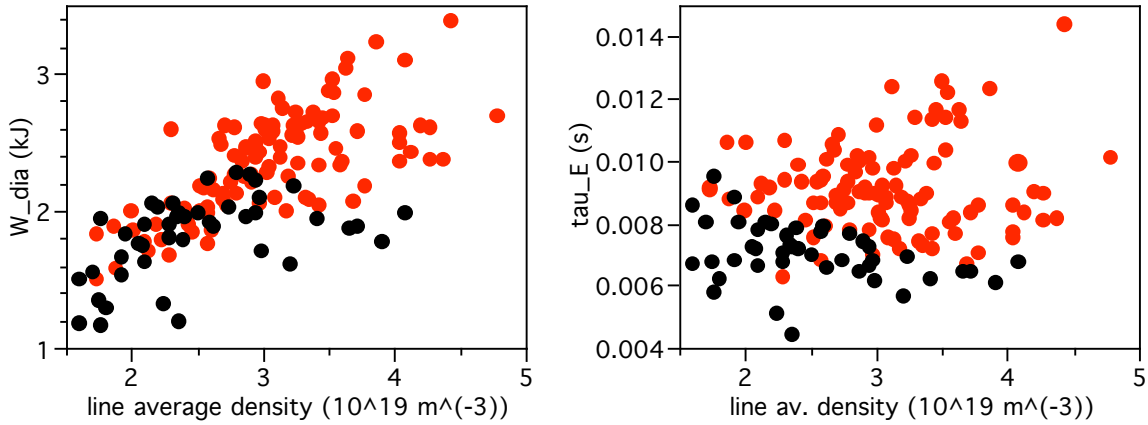

Figure 2: Plasma energy content (left) and energy confinement time (right) vs. plasma density for B-coated (black) Li-coated walls (red symbols).

In boron-coated wall plasmas a systematic, steady density ramp up was observed as the beam power was switched on. This fast density build-up, being limited the available heating power led, generally, to a relatively quick plasma termination due to radiative collapse, for line density values below $4 \times 10^{19} m^{-3}$ [8]. Under lithium conditions this lack of density control has been dramatically improved and long, stationary density plateaus (up to ten average energy confinement times) can be achieved, allowing density scans with the help of external gas puff, as shown in Figure 2. It illustrates the difference between both wall scenarios as regards the behaviour of energy content and confinement time, for NBI discharges using the co-injector with comparable heating power and the same magnetic configuration. It shows that lithium-wall

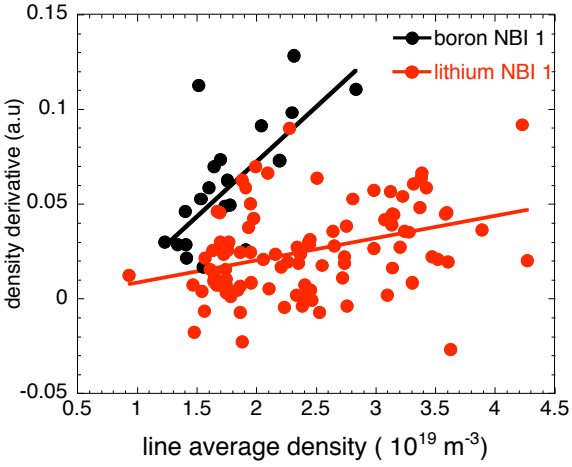

Figure 3: Density increase rate in plasma discharges heated with the co-injector, with B (black) and Li (red symbols) coated walls

coated plasma discharges (red dots) reach higher density values and substantially higher plasma energy content.

Figure 3 displays values of the density slope at a given density for two sets of lithium and boron-coated wall discharges. It shows the drastic reduction of density derivative produced by the lithium wall coating as compared to boron wall conditions. In this more favourable lithium scenario, the plasma tends to evolve spontaneously from a quasi-stationary state with peaked density and radiation profiles to another state with broader profiles and higher density gradients in the outer region. In some occasions, these bifurcations exhibit all the characteristics of the H-mode transition: increase in plasma density and plasma energy content, reduction in the H_α signal, development of steep density gradients and reduction in the turbulence level [9]. But this is not always the case, as discussed in ref. [8], where perturbative experiments are described in which hydrogen and impurity pulses are found to force also a quick change in density and radiation profiles.

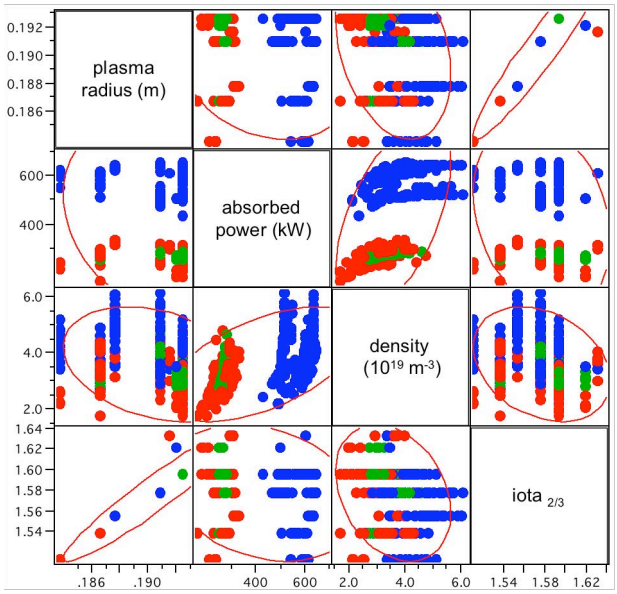

Figure 4: Graphical representation of the studied four-parameter data set with indication of the three types of NBI heating: co- (red), counter (green) and both injectors (blue dots).

Parameter space of the data set

The set of 343 NBI Li-wall plasma discharges has the following distribution: 105 correspond to the co injector, 51 to the counter injector and 187 to simultaneous heating with both. Figure 4 presents the parameter space of the four relevant parameters, plasma radius, absorbed power, density and rotational transform.

The range of variation of plasma radius and rotational transform has been very limited so far. Iota $_{2/3}$ (the value of rotational transform at normalized radius, $\rho = 2/3$) has been changed between 1.51 and 1.64 and plasma radius between 0.18 and 0.19 m. Good coupling of the heating beam to the target plasma has proven to be very challenging for small and indented plasma cross sections, thus precluding the exploration of NBI plasmas in magnetic configurations with small plasma radius or high values of rotational transform. As a consequence, both parameters sets, radius and iota, are highly correlated (correlation 0.95) and therefore not suitable for regression analysis.

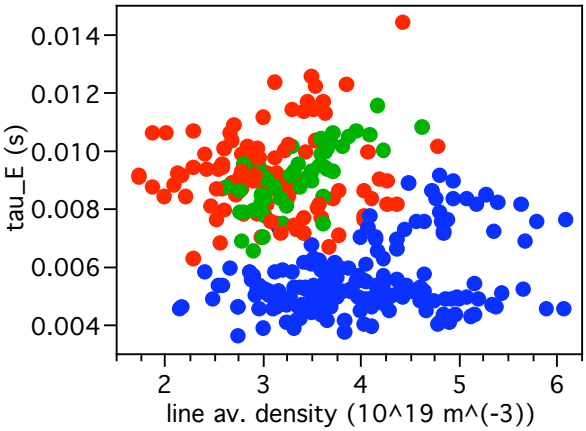

Figure 5: Energy conf. time vs. plasma density for the three types of NBI heating: co (red), counter (green) and both injectors (blue dots).

Plasma density has been varied in the range $1.7\times10^{19}\,m^{-3} \le \bar{n}_e \le 6.1\times10^{19}\,m^{-3}$. The fraction of NBI absorbed power is a function of density in TJ-II. It has been calculated by means of the Fafner II Montecarlo code [6, 10], using electron density and temperature profiles and the

ion temperature, The result yields a value of total estimated absorbed heating power ranging from 160 to 680 kW.

Energy confinement time of the discharges in the data set ranges from 3 to 14 ms, as shown in Figure 5. The energy content values considered for the computation of the confinement are generally taken at the time of maximum energy along the discharge. Thus, the correction to the absorbed power due to the time derivative of the energy can be neglected. Regression analyses of energy confinement on density and heating power yield a scaling law indicating degradation with power, with exponent -0.8 and improvement with density, with exponent 0.5. The density dependence is roughly in line with ISS04 but the power degradation is stronger in the TJ-II case.

Figure 6 shows the experimental energy confinement time versus the ISS04 prediction up shifted by a factor 1.5 to take into account that in this study the diamagnetic energy values are used whereas in the compilation of the ISS04 scaling law [2] TJ-II contributed with the thermal energy values. It is evident that energy confinement in TJ-II is enhanced in NBI plasmas but not as much as Fig. 6 suggests because a new -surely higher- renormalization factor should be calculated and employed for the NBI plasmas of TJ-II.

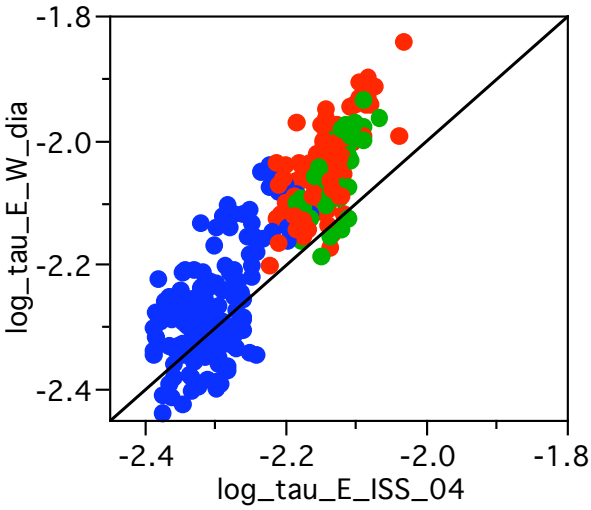

Figure 6: Comparison of the TJ-II NBI experimental energy confinement time with the ISS04 scaling law. Note that the renormalization factor used to downshift the ISS04 prediction, f_{ren} = 0.25, was calculated for TJ-II in ref. [2] and corresponds to ECH plasmas.

References

[1] E. Ascasíbar et al., Nucl. Fusion **45** 276 (2005)
[2] H. Yamada et al., Nucl. Fusion **45** 1684 (2005)
[3] V. I. Vargas et al., Nucl. Fusion **47** 1367 (2007)
[4] F. L. Tabarés et al., Plasma Phys. Control. Fusion **50** 124051 (2008)
[5] J. Sánchez et al., Nucl. Fusion **49** (2009)
[6] J. Guasp et al., "Cálculos de inyección de haces neutros para las descargas de TJ-II". Informes Técnicos Ciemat 1050, Ciemat. Madrid. December 2004
[7] J. M. Fontdecaba et al., "Ion confinement studies in NBI heated TJ-II plasmas using CX-NPA diagnostics" (presented in this Conference)
[8] F. Tabarés et al., " Control of plasma profile by gas and impurity injection in TJ-II under Li wall conditions" (presented in this Conference)
[9] T. Estrada et al., "Physics of sheared flows and transitions to improved confinement regimes in the TJ-II stellarator" (presented in this Conference)
[10] A. Teubel et al., "Montecarlo simulations of neutral beam heating injection into the TJ-II helical axis stellarator". IPP Report 4/268, IPP Garching, March 1994